

NASA TECHNICAL NOTE



NASA TN D-7705

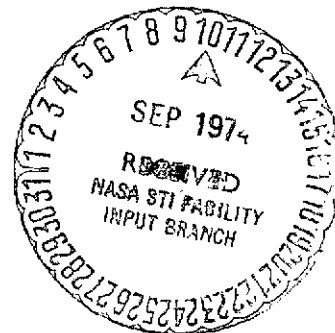
NASA TN D-7705

(NASA-TN-D-7705) EFFECTS OF COMPOSITION  
AND TESTING CONDITIONS ON OXIDATION  
BEHAVIOR OF FOUR CAST COMMERCIAL  
NICKEL-BASE SUPERALLOYS (NASA) 30 p HC  
\$3.25

N74-31985

Unclas  
47132

CSCL 11F H1/17



EFFECTS OF COMPOSITION  
AND TESTING CONDITIONS ON  
OXIDATION BEHAVIOR OF FOUR CAST  
COMMERCIAL NICKEL-BASE SUPERALLOYS

*by Carl E. Lowell and Hubert B. Probst*

*Lewis Research Center  
Cleveland, Ohio 44135*



NATIONAL AERONAUTICS AND SPACE ADMINISTRATION • WASHINGTON, D. C. • AUGUST 1974

1. Report No. NASA TN D-7705		2. Government Accession No.		3. Recipient's Catalog No.	
4. Title and Subtitle EFFECTS OF COMPOSITION AND TESTING CONDITIONS ON OXIDATION BEHAVIOR OF FOUR CAST COMMERCIAL NICKEL-BASE SUPERALLOYS				5. Report Date September 1974	
				6. Performing Organization Code	
7. Author(s) by Carl E. Lowell and Hubert B. Probst				8. Performing Organization Report No. E-7916	
9. Performing Organization Name and Address Lewis Research Center National Aeronautics and Space Administration Cleveland, Ohio 44135				10. Work Unit No. 501-01	
				11. Contract or Grant No.	
12. Sponsoring Agency Name and Address National Aeronautics and Space Administration Washington, D. C. 20546				13. Type of Report and Period Covered Technical Note	
				14. Sponsoring Agency Code	
15. Supplementary Notes					
16. Abstract <p>Four cast nickel-base superalloys were oxidized at 1000° and 1100° C for times up to 100 hr in static air and a Mach 1 gas stream. The oxidation resistance was judged by weight change, metal thickness loss, depletion-zone formation, and oxide formation and morphology. The alloys which formed mostly nickel aluminate (NiAl<sub>2</sub>O<sub>4</sub>) and aluminum oxide (Al<sub>2</sub>O<sub>3</sub>) (B-1900, VIA, and to a lesser extent 713C) were more oxidation resistant. Poorer oxidation resistance was associated with the appearance of chromium sesquioxide (Cr<sub>2</sub>O<sub>3</sub>) and chromite spinel (738X). Refractory-metal content had little effect on oxidation resistance. Refractory metals appeared in the scale as tapiolite (NiM<sub>2</sub>O<sub>6</sub>, where M represents the refractory metal). Thermal cycling in static air appeared to supply sufficient data for the evaluation of oxidation resistance, especially for alloys which form oxides of low volatility. For alloys of higher chromium levels with high propensities toward forming a chromium-bearing scale of higher volatility, testing under conditions of high gas velocity is necessary to assess fully the behavior of the alloy.</p>					
17. Key Words (Suggested by Author(s)) Oxidation; Superalloys; Nickel base; Oxides			18. Distribution Statement Unclassified - unlimited Category 17		
19. Security Classif. (of this report) Unclassified		20. Security Classif. (of this page) Unclassified		21. No. of Pages 28	
				22. Price* \$3.25	

# EFFECTS OF COMPOSITION AND TESTING CONDITIONS ON OXIDATION BEHAVIOR OF FOUR CAST COMMERCIAL NICKEL-BASE SUPERALLOYS

by Carl E. Lowell and Hubert B. Probst

Lewis Research Center

## SUMMARY

The alloys chosen are NASA VIA, B-1900, 713C, and 738X. They represent current cast nickel-base turbine alloys. Their compositions provided reasonable ranges of the alloying elements expected to affect oxidation behavior: aluminum, chromium, titanium, and refractory metals. The alloys were exposed to 1000° and 1100° C air in furnaces and a Mach 1 burner. Alloys were tested isothermally and cyclically for 100 hours. Oxidation behavior was judged by kinetics, microstructures, and X-ray diffraction. All test methods ranked VIA and B-1900 best, followed by 713C and 738X. Better oxidation resistance was associated with aluminum-rich scale formation; poorer oxidation resistance was associated with chromium-rich scales. Refractory-metal content was not detrimental to oxidation resistance. Although oxides of refractory metals can be volatile, in these tests they formed a nonvolatile oxide, tapiolite ( $\text{NiM}_2\text{O}_3$ ). Thermal cycling resulted in some loss in oxidation, especially in the furnace tests of 713C and 738X. The effect of high gas velocity was to accelerate the oxidation of chromium-rich scale forming alloys. Gas velocity had little effect on aluminum-rich scales. High-gas-velocity testing is not necessary to obtain a realistic evaluation of alloys that form nonvolatile scales. Valid comparisons of such alloys can be obtained by lower cost furnace testing. However, alloys forming volatile scales do require high-velocity testing.

## INTRODUCTION

There has been a continuing interest in increasing the operating temperature of gas turbine engines in order to achieve higher efficiencies and the attendant benefits which accompany such efficiency increases. In answer to this demand, nickel (Ni)-base superalloys have been steadily improved over the years to provide the required high-temperature mechanical properties. These improvements have been achieved primarily by increasing the amounts of strengthening elements, for example, aluminum (Al), titanium (Ti), and refractory metals. These increases have been accommodated usually by lowering chromium (Cr) contents below 20 percent

and have often resulted in lower levels of oxidation resistance.

While coatings have provided a practical means to circumvent the oxidation limitations of alloys, there still remains a need to understand the oxidation behavior of the alloys themselves. This is certainly apparent with respect to the direct influence of alloy chemistry on oxidation behavior and the possibility of developing alloys of improved oxidation resistance. However, the various manifestations of oxidation that can contribute to the degradation of mechanical properties and the effects that test parameters can exert on the apparent oxidation behavior are more subtle.

Considering only one mechanical property as an example, oxidation can reduce load carrying capability in a number of ways. Straightforward metal consumption by conversion to oxide scales is an obvious means. Also, depletion of strengthening elements from regions adjacent to oxidation reaction sites and/or rapid grain boundary attack could contribute to reduced strength. However, classical oxidation measurements such as weight change shed little light on the degree to which such damaging reactions have occurred.

Understanding alloy oxidation relevant to a given intended use of the alloy presents questions as to what tests are needed, their merits, and their relative severity. While isothermal testing is most commonly used, as seen in the recent oxidation surveys of reference 1, it falls far short of providing all the environmental features that can affect oxidation in a gas turbine engine. Introducing a cyclic heating schedule results in conditions more closely approaching those in an engine (ref. 2), but the inclusion of a high gas velocity as is done in so-called burner rigs (ref. 3) provides a better simulation. This much is evident, but the question of the relation among the different tests is still open. These relations must be addressed if we are to be able to choose the proper test or sequence of tests in order to evaluate correctly the behavior of an alloy or the effects of specific test parameters.

Thus, the present investigation was initiated in order to make a comprehensive comparative study of the behavior of several cast nickel-base superalloys when subjected to a variety of oxidation tests. These include isothermal tests, cyclic tests, and high-velocity tests. The primary objectives of this program were to identify the oxidation processes that are predominant in these tests for several typical cast alloys, to rank the alloys, and to relate their oxidation behavior to alloy chemistry. A secondary goal was to understand the relation of the tests to one another as to severity and changes in mode of oxidation that occur.

The alloys chosen for this study were VIA, B-1900, 713C, and 738X. These alloys were chosen as typical of current technology. Alloys VIA and B-1900 represent the strongest cast alloys with large volume fractions of  $\gamma'$ . Alloy 713C is one of more moderate strength levels. Alloy 738X is an alloy of high Cr content known for its good resistance to hot corrosion (i.e., accelerated oxidation associated with the presence of sodium sulfate ( $\text{Na}_2\text{SO}_4$ )). In selecting commercial compositions, systematic variation of selected alloying elements is, of course, not possible. However, these four alloys offer fairly wide ranges in the variation of the major alloying elements most likely to affect oxidation behavior. Within the four alloys the approximate ranges of composition (in wt. %) are as follows: Cr, 6 to 16; Al, 3.5 to 6; Ti, 1 to 3.5; Co, 0.5 to 10; and refractory metals, 6.5 to 18 (tables I and II). Further, some alloy comparisons allow a determination of the effects of specific alloy additions on oxidation. For example, the major difference in the compositions of VIA and B-1900 is the refractory-metal content, 17.9 percent in VIA as compared to 10.3 percent in B-1900. The Al and Ti contents of B-1900 and 713C are nearly the same, while the refractory-metal and Cr contents differ. Alloys 713C and 738X have nearly the same Cr and refractory-metal contents, but differ in the amount of Al and Ti.

The results of this program are presented in separate NASA reports that cover specific portions of this program. They deal with

- (1) Cyclic and isothermal furnace data (ref. 4)
- (2) High-temperature X-ray diffraction (HTXRD) of the oxides as they form (ref. 5)
- (3) High-gas-velocity oxidation (ref. 6)
- (4) An analysis of the relations of the first three items and their implication for further work

This report deals with the last part of the program. It summarizes the cyclic and isothermal oxidation of the four alloys, both in furnace and in high-velocity tests; ranks the alloys; shows relations between alloy chemistry and oxidation behavior; and defines relations among the various testing parameters.

## MATERIALS AND SPECIMEN PREPARATION

Samples used in furnace testing and HTXRD were commercially cast as approximately 2.5- by 0.64- by 10.2-centimeter bars. These were cut to the shapes shown in

figures 1(a) and (b), and the surfaces were glass-bead blasted. The high-velocity test bars were cast to approximately the size and shape shown in figure 1(c), except for the grooves. All samples were given the heat treatments they would normally receive for commercial use: VIA, 32 hours at 900<sup>0</sup> C in argon; B-1900, 4 hours at 1080<sup>0</sup> C in argon; 713C, no treatment; and 738X, 2 hours at 1120<sup>0</sup> C in argon. Cooling from these temperatures was in argon at a rate equivalent to air cooling. The grooves were cut, and the samples were machined to final size after being heat treated. The machining was followed by glass-bead blasting.

Chemical analyses were made on each alloy, and the results are shown in table II. All values are within the established specifications for these alloys. Figure 2 shows that all four alloys have the microstructure commonly associated with cast nickel-base superalloys containing the  $\gamma'$  phase.

## APPARATUS AND TEST PROCEDURES

The details of the apparatus and procedures are discussed completely in other publications (refs. 4 to 6). They are summarized in this section.

All furnace testing was done in static air; the experimental apparatus is described in reference 4 and shown schematically in figure 3. The isothermal testing consisted of a continuous recording of weight change at temperature with a precision of  $\pm 0.2$  milligram. Weight changes of thermally cycled samples were determined at convenient times at room temperature with the same precision. Temperatures were held at  $\pm 5^{\circ}$  C. Cyclic testing consisted of exposures for 1 hour in the furnace and 40 minutes of cooling per cycle. In both cyclic and isothermal tests spall was collected and analyzed after cooling.

High-temperature X-ray diffraction studies consisted of taking sequential diffractograms at temperature and measuring the peak heights of unambiguous lines from each oxide phase (ref. 5). These peak intensities were normalized and plotted against time. The samples were heated on a platinum strip heater (fig. 4). Sample temperatures were controlled to  $\pm 3^{\circ}$  C.

High-gas-velocity oxidation was achieved by exposing the samples to a Mach 1 combustion gas stream produced by burning Jet A fuel (ref. 6). The burner required for these exposures is shown in figure 5. A cycle consisted of 1 hour in the jet stream followed 3 minutes in a Mach 1 cold air stream. Isothermal testing con-

sisted of heating in 15-hour increments followed by cooling in still air overnight. In both cases the temperature was held to  $\pm 15^{\circ}$  C, and the samples were weighed at room temperature to a precision of  $\pm 0.2$  milligram.

After exposure all samples were subjected to metallographic and X-ray diffraction analysis. Furnace and high-velocity test specimens were also analyzed for metal loss and depletion-zone formation. Metal loss data are obtained by measuring the distance across the sample from scale-metal interface to scale-metal interface and subtracting this value from the original metal thickness.

## RESULTS

Four nickel-base superalloys (VIA, B-1900, 713C, and 738X) were oxidized at  $1000^{\circ}$  and  $1100^{\circ}$  C in air isothermally and cyclically. Oxidation testing was carried out in a high-temperature diffractometer, a static furnace, and a Mach 1 burner rig. The results of these tests are discussed in this section.

### Oxidation Products

The oxides found on the surfaces of the alloys and in their spalls were similar inasmuch as they generally included as major phases aluminum oxide ( $\text{Al}_2\text{O}_3$ ), several spinels, chromium sesquioxide ( $\text{Cr}_2\text{O}_3$ ), and tapiolite ( $\text{NiM}_2\text{O}_6$ ). (This phase is essentially nickel tantalate ( $\text{NiTa}_2\text{O}_6$ ), nickel niobate ( $\text{NiNb}_2\text{O}_6$ ), or a mixture of both. While large amounts of tungsten (W) or molybdenum (Mo) or both may be substituted for tantalum (Ta) or niobium (Nb), this structure cannot be produced without either Ta or Nb.) The main differences among the alloys were the relative amounts of each of the oxides, especially the sesquioxide and spinels.

Figure 6 is taken from reference 5 and shows the oxide development as a function of time at  $1100^{\circ}$  C under both cyclic and isothermal oxidation of VIA and 738X.

The results for VIA are very similar to those for B-1900 and not much different from those for 713C. Cycling had little effect on the order of oxide formation, but did reduce the amount of retained oxide as a result of spalling.

Both B-1900 and VIA developed oxides with high Al content. The two major oxides were nickel aluminate ( $\text{NiAl}_2\text{O}_4$ ) and  $\text{Al}_2\text{O}_3$ . In addition, substantial amounts of tapiolite were always present. While some nickel monoxide ( $\text{NiO}$ ) or  $\text{Cr}_2\text{O}_3$  was

present occasionally, they were always minor phases.

As the Cr content of the alloys increased, less  $\text{Al}_2\text{O}_3$  was observed and more  $\text{Cr}_2\text{O}_3$ . Concurrently, the spinels on the alloys with higher Cr content contained more nickel chromite ( $\text{NiCr}_2\text{O}_4$ ), and greater amounts of NiO developed. This tendency to form Cr-bearing oxides is most pronounced on 738X, while considerably lesser amounts of Cr-bearing oxides are present on 713C. The amounts of tapiolite formed were generally less on 713C and 738X and corresponded to their refractory-metal contents, which are lower than those of VIA and B-1900.

### Weight Change Data

A summary of the 100-hour weight change data is presented in table III. Selected kinetic curves are shown in figures 7 and 8. The isothermal furnace values in table III are not the values of test temperature usually presented. They are values obtained after cooling the samples to room temperature at the conclusion of the test. This allows a direct comparison with isothermal burner rig samples, which cannot be weighed at temperature.

Furnace testing of VIA, B-1900, and 713C resulted in little weight change, less than 1 milligram per square centimeter. In contrast, 738X changed weight by more than 1 milligram per square centimeter under all test conditions and reached a maximum change of 27.56 milligrams per square centimeter lost at  $1100^\circ\text{C}$  during cyclic oxidation. The curves of weight change as a function of time for the four alloys tested in static air at  $1100^\circ\text{C}$  isothermally and cyclically shown in figure 7 give a graphic comparison of the behavior of the alloys. Alloys VIA and B-1900 behave similarly in that weight changes are small and there is comparatively little difference between isothermal and cyclic behavior. Alloy 713C shows a more obvious difference between isothermal and cyclic oxidation. During isothermal exposure 713C gains some weight; however, during cycling it loses weight. The greatest difference between isothermal and cyclic oxidation behavior is exhibited by 738X. It undergoes considerable weight gain during isothermal exposure and suffers severe weight loss upon cycling.

The high-velocity weight change data are given in figure 8. A comparison of weight change under high-gas-velocity conditions and static furnace conditions for all five alloys is summarized in table III. The weight change behavior of alloys 713C and 738X is most drastically affected by high gas velocity, while that of VIA and



B-1900 is only minimally affected.

### Thickness Change Data

Two sets of measurements are presented in table IV and figures 9 and 10, metal and depletion-zone thickness changes. The metal thickness change data were obtained by measuring the distance across the sample from scale-metal interface to scale-metal interface and subtracting this value from the metal thickness prior to testing. These data are subject to about a 10-micrometer error (ref. 4), and no values less than 10 micrometers are listed. After all modes of testing all samples had microstructures which contained a measurable depletion zone (e.g., figs. 11 and 12). The error in the depletion-zone thickness was less, since its determination does not require a correlation of measurements before and after oxidation (see refs. 4 and 6 for greater detail). The exact relation of depletion zone to oxidation attack is unclear, but larger depletion zones indicate greater oxidation attack. The depletion zones were obviously free of  $\gamma'$ , which indicated a loss of Al; however, it is likely that other alloying elements were also lost. The existence of a zone depleted in Al will certainly degrade oxidation resistance in addition to lowering strength, since the major strengthening phase ( $\gamma'$ ) is absent. In judging the data one must consider the sum of both metal thickness change and depletion-zone thickness.

The thickness change data are presented in table IV and figures 9 and 10. As in the case of the weight change measurements, alloys VIA and B-1900 showed the least attack. Similar thickness losses were obtained in furnace and high-velocity tests for both alloys. In contrast, 738X exhibited considerable thickness loss, in both the furnace and high-velocity-gas exposures. The thickness losses suffered by 713C were intermediate between those of 738X and VIA and B-1900. The effect of high gas velocity on thickness change is more apparent in alloys 738X and 713C than in VIA and B-1900.

## DISCUSSION

### Alloy Chemistry Effects

An evaluation of all tests leads one to the conclusion that 738X has clearly the poorest oxidation resistance. Alloy 713C has somewhat greater oxidation resistance,

but has oxidation resistance substantially poorer than that of B-1900 and VIA. Thus, the alloys of greatest oxidation resistance, B-1900 and VIA, are those with the most Al and refractory-metal content and the least Cr content. The chemistry differences are related to the oxides formed on these alloys. Alloys B-1900 and VIA formed mainly  $\text{Al}_2\text{O}_3$ , Al-rich spinels, and tapiolite. Alloy 713C shows a tendency for more Cr in the spinels and more  $\text{Cr}_2\text{O}_3$ , while 738X, the alloy with the highest Cr content, oxidized to Cr-rich spinels and substantial amounts of  $\text{Cr}_2\text{O}_3$ . The amount of tapiolite formed seemed roughly proportional to the refractory-metal content, as might be expected.

The preferential formation of  $\text{Al}_2\text{O}_3$  and Al-rich spinels was obviously associated with the aluminum content, as demonstrated by the oxidation of VIA and B-1900. However, Al content was not the sole factor, as is illustrated by the fact that 713C, which contained the same amount of Al as B-1900 and slightly more than VIA, had less tendency for  $\text{Al}_2\text{O}_3$  formation than B-1900 or VIA.

Barrett and Lowell (ref. 7) have shown that sensitivity to cyclic oxidation increases with increasing Cr contents in wrought superalloys, and this observation is confirmed in the present work on cast  $\gamma$ - $\gamma'$  alloys. In reference 7 the cyclic oxidation resistance was correlated with chromite and aluminate spinel concentrations, greater resistance to cyclic oxidation being associated with higher concentrations of aluminate spinel and lower amounts of chromite spinel. This same correlation is now suggested for the cast alloys studied.

The fact that the oxidation of 713C and 738X was accelerated by high-velocity testing, especially at  $1000^\circ\text{C}$ , while VIA and B-1900 were only slightly affected also appears to be related to Cr content. Kohl and Stearns (ref. 8) calculated and Lowell and Sanders (ref. 9) and Graham and Davis (ref. 10) confirmed experimentally that Cr-containing oxides, especially  $\text{Cr}_2\text{O}_3$ , are quite volatile. The effect of this volatility, which involves the reaction  $\text{Cr}_2\text{O}_3 + \text{O}_2 \rightarrow \text{CrO}_3 \uparrow$ , is to be greatly accelerated by the gas velocity, as is shown in figure 13.

Although simple refractory-metal oxides, for example, molybdenum trioxide ( $\text{MoO}_3$ ), are known to be volatile, the alloys with the higher W and Mo contents, B-1900 and particularly VIA, did not suffer serious weight losses under high-velocity testing. This effect appears to be due to the formation of tapiolite as the only oxide phase containing refractory metals. Whether this oxide is beneficial is uncertain, but it is probably neither volatile nor harmful, inasmuch as the alloys with the greatest amount of this oxide were the most oxidation resistant.

The role of Ti is not clear. Only in oxidized 738X was a Ti-bearing oxide identified (nickel titanate ( $\text{NiTiO}_3$ )). Also, 738X contained by far the most Ti (3.4 wt. %).

In brief, then, the most important elements to consider in oxidation resistance are Al and Cr. However, it should not be assumed that the Al and Cr contents in the alloy alone will enable one to judge the potential oxidation resistance of an alloy. It is quite likely that the distribution of Al and Cr between  $\gamma$  and  $\gamma'$  may be more important. In the case of the  $\gamma'$  phase, one would wish as low a Cr level as possible, since this element drastically reduced the cyclic oxidation resistance of  $\gamma'$  (ref. 11). On the other hand, the most oxidation resistant  $\gamma$  alloy would be one of the type Ni-Cr-Al, where the Cr level would be 15 to 20 weight percent and the Al level would be 4 to 6 weight percent (ref. 12). An alloy with such phase compositions might offer enough oxidation resistance to be used without coating at temperatures in excess of  $1100^\circ\text{C}$ . It is not, at present, known whether or not such phase compositions would be stable. However, the work of Kriege and Baris (ref. 13) on the partitioning of elements in  $\gamma$ - $\gamma'$  alloys indicates that compositions near the desired one are reached in such alloys as B-1900.

### Testing Condition Effects

The effects of thermal cycling and velocity were straightforward with these alloys. The effect of thermal cycling was to accelerate oxidation attack and accentuate the differences among the alloys. Thermal cycling reduces the protection of the oxide layer by causing spalling when the specimen is cooled after each cycle. This phenomenon is not well understood but is apparently due to stresses induced by thermal expansion differences between the alloy and the scale. With minor exceptions, the ranking without cycling was the same as that with cycling. This behavior has been noted with other alloys, especially aluminum oxide formers (ref. 7).

As with thermal cycling, the effect of high gas velocity increased the rate of attack but did not change the ranking of the alloys. This behavior occurs because the volatile oxide-forming alloys (713C and 738X) also have the greater furnace isothermal oxidation rates. Some alloys would not behave in this fashion. For example, TD-NiCr has a low isothermal oxidation rate, but forms a volatile oxide,  $\text{Cr}_2\text{O}_3$ . In furnace tests it has excellent oxidation resistance, but in high-velocity testing loses weight rapidly (ref. 9).

Which test one uses for a given alloy should, therefore, be decided on a knowledge of what oxides may be expected. In most cases a ranking of alloys may be obtained by furnace testing, cyclically to increase differences. However, to determine more closely the amount of attack one might expect under turbine conditions, the use of high-velocity testing would be required for those alloys forming a volatile oxide. Therefore, for many alloys cyclic furnace testing alone is sufficient to give data reliable to use conditions.

### CONCLUDING REMARKS

An attempt should be made to develop an oxidation-resistant  $\gamma$ - $\gamma'$  alloy. This alloy might be developed by making compositional modifications to produce a  $\gamma'$  phase with minimum Cr and a  $\gamma$  phase with a composition similar to current Ni-Cr-Al coatings. The resultant alloy should have highly oxidation resistant phases and might be used uncoated at temperatures of 1100° C and above. If a high refractory-metal content proves necessary for mechanical-property requirements, Ta and Nb would probably be the preferred choices. These elements would most likely lead to tapiolite formation during oxidation. This oxide has been shown to be not detrimental to oxidation resistance.

### CONCLUSIONS

Four nickel-base complex high-temperature  $\gamma'$ -strengthened cast superalloys (VIA, B-1900, 713C, and 738X) were isothermally and cyclically oxidized at 1000° and 1100° C in static air and Mach 1 combustion products. These alloys are representative of high-temperature,  $\gamma'$ -strengthened alloys of complex chemistry. Oxide phases formed were identified with the aid of high-temperature X-ray diffraction. Comparative oxidation behavior was evaluated by using weight change, thickness change, and metallography. On the basis of these tests the following conclusions appear justified for these four alloys:

## Chemistry Effects

1. Alloys B-1900 and VIA had the best overall oxidation resistance, 713C less resistance, and 738X the least resistance.
2. Good oxidation resistance appeared to be related to the formation of aluminum oxide and aluminate spinel, while poor resistance was accompanied by chromium sesquioxide and chromite spinel.
3. The more oxidation resistant alloys were high in aluminum and refractory metals and low in chromium, the reverse of the alloys with poorer oxidation resistance. Thus, the loss of oxidation resistance resulting from lowering chromium concentrations, from 20 to a range of 6 to 16 percent, may be more than offset by increases in aluminum content.
4. The refractory metals oxidized to a tapiolite structure ( $\text{NiM}_2\text{O}_6$ ), which was not detrimental.

## Test Effects

1. The effect of thermal cycling on furnace testing is to give a more realistic estimate of the amount of attack under real conditions, but it does not change the ranking of alloys.
2. The oxidation rate of those alloys that form volatile oxides, for example, chromium-bearing alloys, was accelerated by high-velocity burner rig testing. The velocity effect was not particularly significant for alloys that did not form chromium-bearing oxides as a major scale, especially alloys that form aluminum oxide.
3. For alloys which do not form substantial amounts of volatile oxides (low-chromium alloys), it appears that cyclic furnace testing may provide sufficient oxidation information. High-velocity burner rig testing may not be a necessity. Thus, a brief, isothermal furnace exposure followed by X-ray diffraction analysis can be used to identify those alloys forming chromium-rich scales which would require high-velocity testing.

Lewis Research Center,  
National Aeronautics and Space Administration,  
Cleveland, Ohio, April 23, 1974,  
501-01.

## REFERENCES

1. Wright, I. G.: Oxidation of Iron-, Nickel-, and Cobalt-Base Alloys. MCIC-72-07, Batelle Columbus Labs., Materials and Ceramics Information Center (AD-745473), 1972.
2. Grisaffe, Salvatore J; and Lowell, Carl E.: Examination of Oxide Scales on Heat Resisting Alloys. NASA TN D-5019, 1969.
3. Johnston, James R.; and Ashbrook, Richard L.: Oxidation and Thermal Fatigue Cracking of Nickel- and Cobalt-Base Alloys in a High Velocity Gas Stream. NASA TN D-5376, 1969.
4. Barrett, Charles A.; Santoro, Gilbert J.; and Lowell, Carl E.: Isothermal and Cyclic Oxidation at 1000<sup>o</sup> and 1100<sup>o</sup> C of Four Nickel-Base Alloys: NASA-TRW VIA, B-1900, 713C, and 738X. NASA TN D-7484, 1973.
5. Garlick, Ralph G.; and Lowell, Carl E.: Alloy Composition Effects on Oxidation Products of VIA, B-1900, 713C, and 738X: A High Temperature Diffractometer Study. NASA TM X-2796, 1973.
6. Sanders, William A.: Dynamic Oxidation Behavior at 1000<sup>o</sup> and 1100<sup>o</sup> C of Four Nickel-Base Cast Alloys, NASA-TRW VIA, B-1900, 713C, and 738X. NASA TN D-7682. 1974.
7. Barrett, Charles A.; and Lowell, Carl E.: Comparison of Isothermal and Cyclic Oxidation Behavior of Twenty-Five Commercial Sheet Alloys at 1150<sup>o</sup> C. NASA TN D-7615, 1974.
8. Kohl, Fred J.; and Stearns, Carl A.: Vaporization of Chromium Oxides from the Surface of TD-NiCr under Oxidizing Conditions. NASA TM X-52879, 1970.
9. Lowell, Carl E.; and Sanders, William A.: Mach 1 Oxidation of Thoriated Nickel Chromium at 1204 C (2200<sup>o</sup> F). Oxidation of metals, vol. 5, no. 3, Dec. 1972, pp. 221-239.
10. Graham, H. G.; and Davis, H. H.: Oxidation/Vaporization Kinetics of Cr<sub>2</sub>O<sub>3</sub>. J. Am. Ceram. Soc., vol. 54, Feb. 1971, pp. 89-93.

11. Santoro, Gilbert J.; Deadmore, Daniel L.; and Lowell, Carl E.: Oxidation of Alloys in Nickel-Aluminum System with Third Element Additions of Chromium, Silver, and Titanium at 1100 C. NASA TN D-6414, 1971.
12. Giggins, C. S.; and Pettit, F. S.: Oxidation of Ni-Cr-Al Alloys between 1000 and 1200 C. J. Electr. Chem Soc., vol. 118, Nov. 1971, pp. 1782-1790.
13. Kriege, Owen H.; and Baris, J. M.: The Chemical Partitioning of Elements in  $\gamma'$  Separated from Precipitation-Hardened, High-Temperature Nickel-Base Alloys. ASM Trans. Quart., vol. 62, Mar. 1969, pp. 195-200.

TABLE I. - KEY ELEMENT CONTENT OF FOUR NICKEL-BASE ALLOYS

Alloy	Chromium	Aluminum	Titanium	Refractory metals		
				Total	Molybdenum, tungsten, and rhenium (a)	Tantalum and niobium (b)
				Concentration, wt. %		
VIA	5.9	5.3	1.0	17.9	8.4	9.5
B-1900	8.0	6.2	1.1	10.3	6.1	4.2
713C	13.6	6.0	.9	6.3	4.2	2.1
738X	15.8	3.6	3.4	7.0	4.5	2.5

<sup>a</sup>As pure metals which form volatile oxides at elevated temperatures.

<sup>b</sup>As pure metals which form porous oxides at elevated temperatures.

TABLE II. - CHEMICAL ANALYSIS OF FOUR  
NICKEL-BASE ALLOYS

Element	Alloy			
	VIA	B-1900	713C	738X
	Concentration, wt. %			
Chromium	5.86	7.99	13.64	15.84
Cobalt	7.24	10.00	.53	8.81
Aluminum	5.27	6.18	6.00	3.57
Titanium	.95	1.11	.87	3.39
Boron	.021	.014	.009	.01
Zirconium	.10	.06	.10	.08
Carbon	.11	.12	.13	.16
Tantalum	9.03	4.14	(a)	1.68
Niobium	.45	<.05	(a)	.85
Molybdenum	2.11	6.05	4.18	1.70
Tungsten	5.96	<.05	NA <sup>b</sup>	2.78
Iron	.08	<.10	.39	<.10
Rhenium	.32	NA	NA	NA
Hafnium	.39	NA	NA	NA
Copper	<.05	NA	<.10	<.08
Manganese	.02	<.02	<.05	<.02
Sulfur	.008	.007	.009	.006
Silicon	<.10	<.05	.17	<.50
Nickel	Remainder	Remainder	Remainder	Remainder

<sup>a</sup>Ta + Nb = 2.10.

<sup>b</sup>Not analyzed.



TABLE III. - SPECIFIC WEIGHT CHANGE AFTER 100 HOURS

[All values taken at room temperature.]

Alloy	Furnace				Burner rig			
	Isothermal		Cyclic		Isothermal		Cyclic	
	1000° C	1100° C	1000° C	1100° C	1000° C	1100° C	1000° C	1100° C
	Specific weight change, mg/cm <sup>2</sup>							
VIA	0.41	0.89	0.51	-0.67	0.34	-2.74	0.67	-3.41
B-1900	.21	.16	.25	-.59	.26	-1.54	.66	-1.97
713C	.25	-.25	.32	-4.70	-4.61	-9.48	-3.16	-8.43
738X	1.81	-1.11	2.72	-27.56	-11.9	-38.1	-13.4	-115.6

TABLE IV. - THICKNESS CHANGES AFTER 100 HOURS OF OXIDATION

Alloy	Furnace								Burner rig							
	Isothermal				Cyclic				Isothermal				Cyclic			
	1000° C		1100° C		1000° C		1100° C		1000° C		1100° C		1000° C		1100° C	
	Metal	Depletion zone	Metal	Depletion zone	Metal	Depletion zone	Metal	Depletion zone	Metal	Depletion zone	Metal	Depletion zone	Metal	Depletion zone	Metal	Depletion zone
	(a)	(b)	(a)	(b)	(a)	(b)	(a)	(b)	(a)	(b)	(a)	(b)	(a)	(b)	(a)	(b)
Thickness change, $\mu\text{m}$																
VIA	NS	7	NS	14	NS	7	NS	14	NS	8	NS	30	NS	10	NS	24
B-1900	NS	6	NS	10	NS	4	NS	7	NS	7	NS	15	NS	6	NS	19
713C	NS	8	NS	22	NS	7	14	30	15	48	NS	39	NS	51	NS	49
738X	NS	30	NS	60	12	27	50	111	29	22	55	123	51	21	140	55

<sup>a</sup>Values  $\leq 10 \mu\text{m}$  are considered not significant (NS).<sup>b</sup>Values are accurate to  $\pm 2 \mu\text{m}$ .

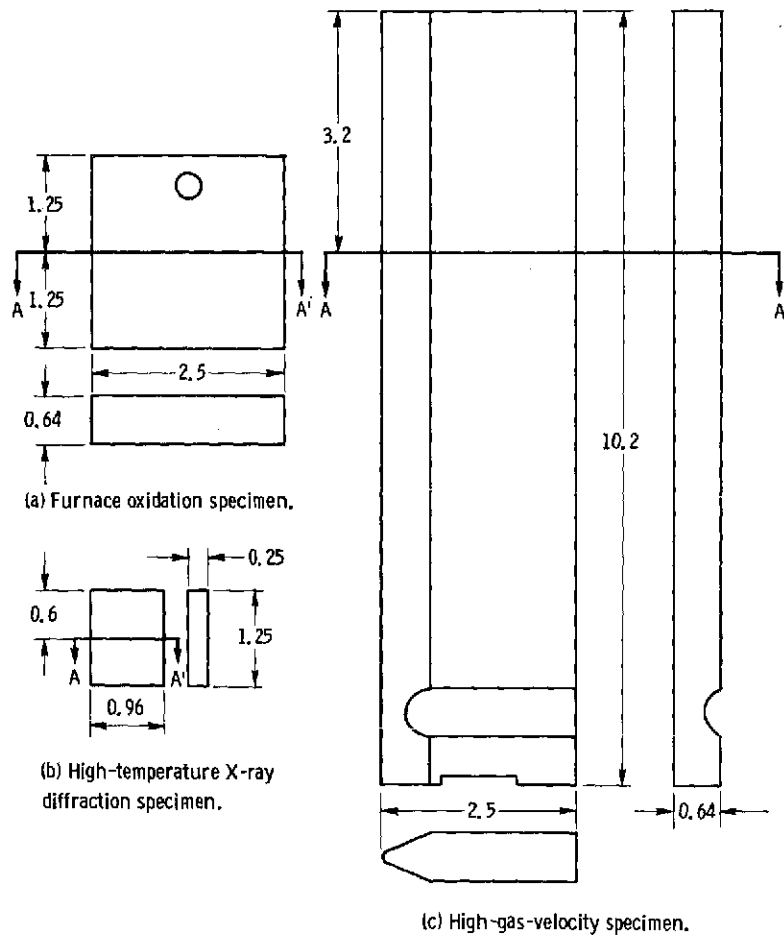
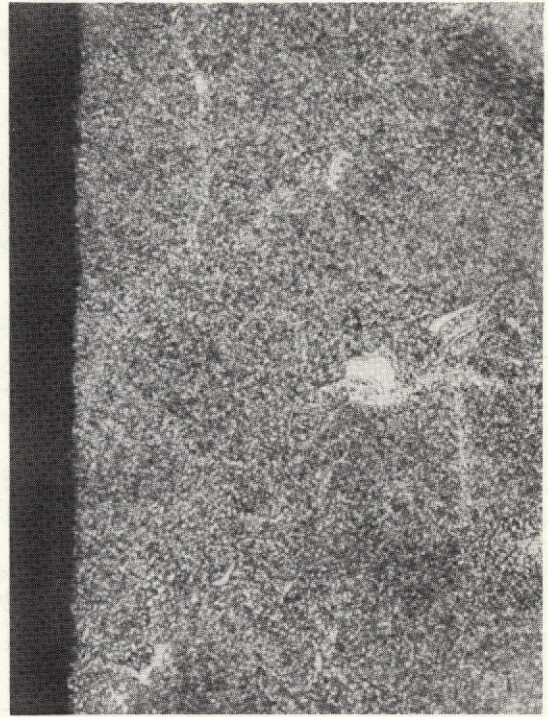


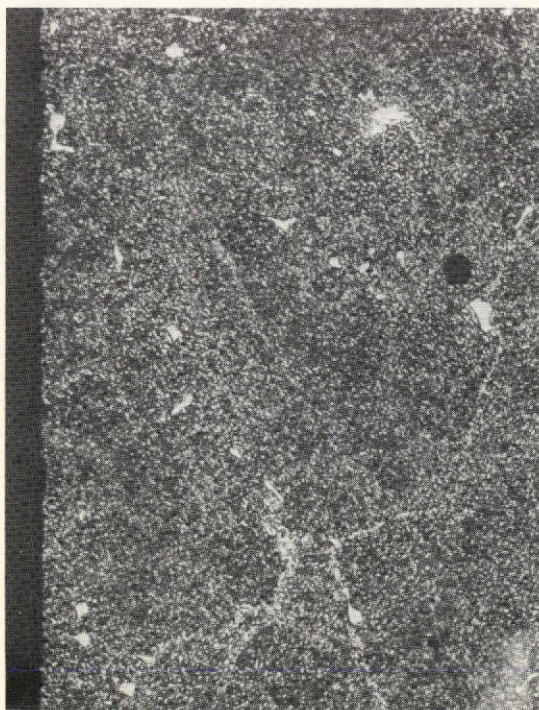
Figure 1. - Sample geometries and sectioning planes of oxidation samples. Metallographic sections made at A - A'. (Dimensions in centimeters.)



(a) VI A.



(b) B-1900.



(c) 713C.



(d) 738X.

Figure 2. - Microstructures of as-cast alloys. Etchant: 33 percent water, 33 percent nitric acid, 33 percent acetic acid, and 1 percent hydrofluoric acid. X250.



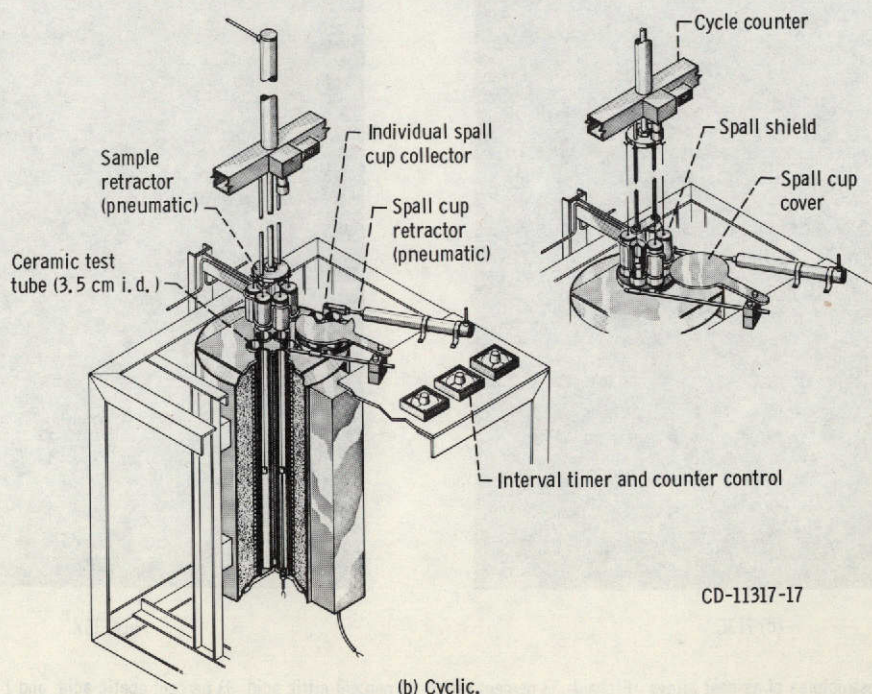
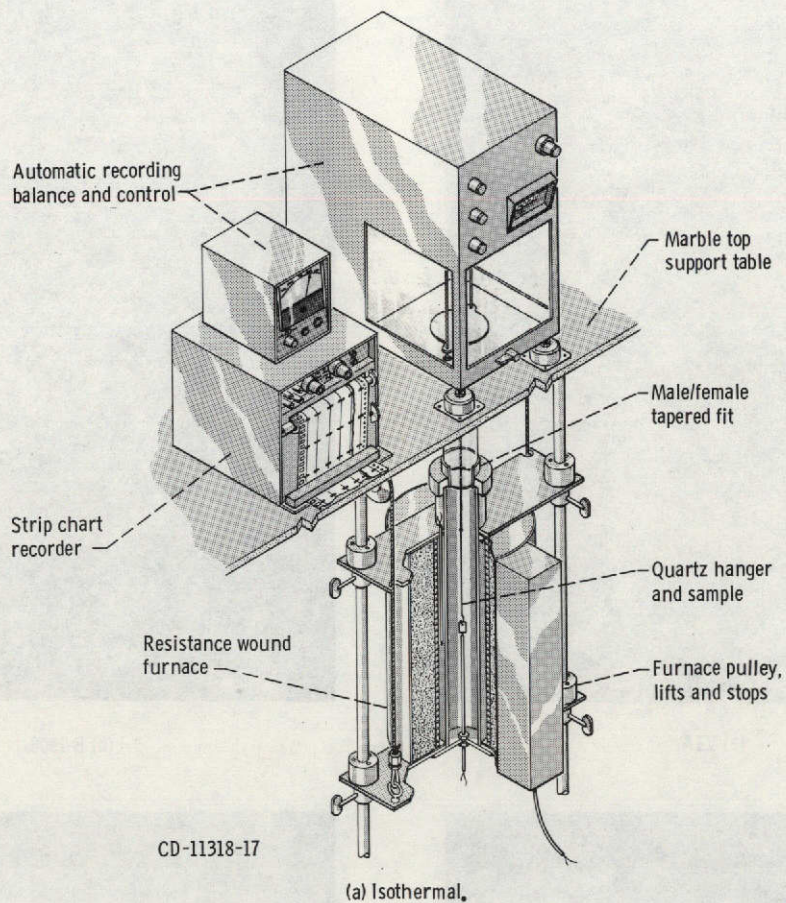


Figure 3. - Oxidation apparatus.



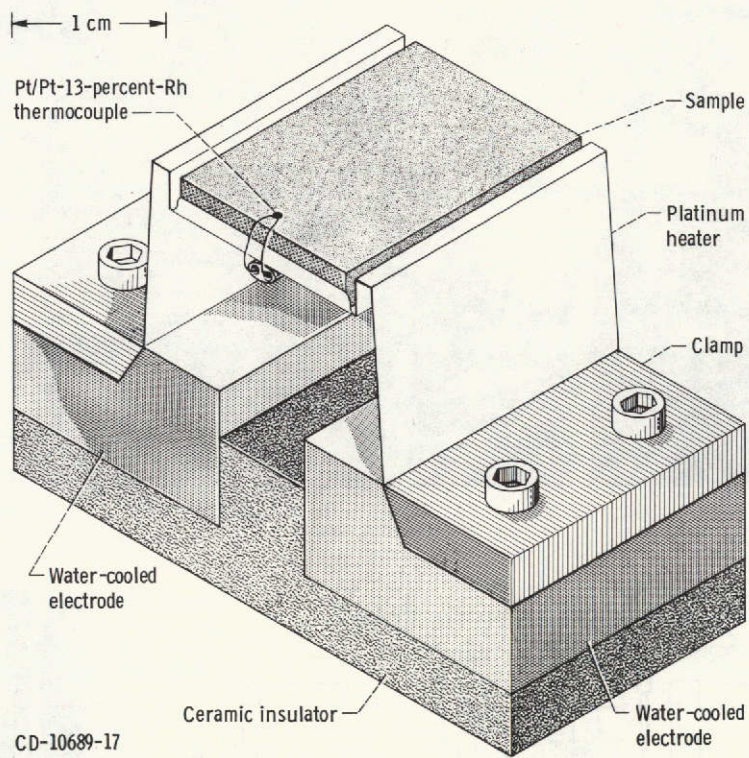
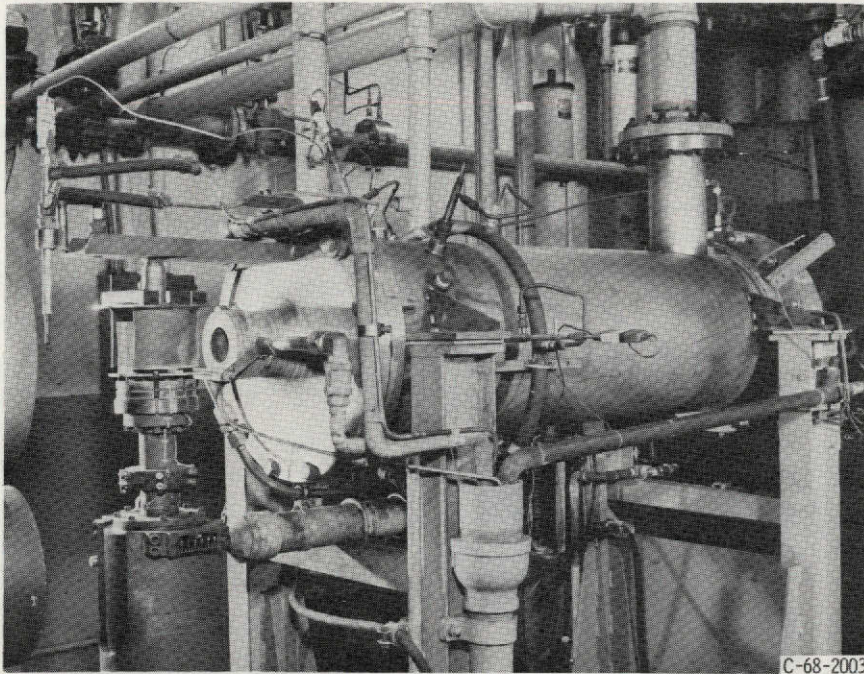


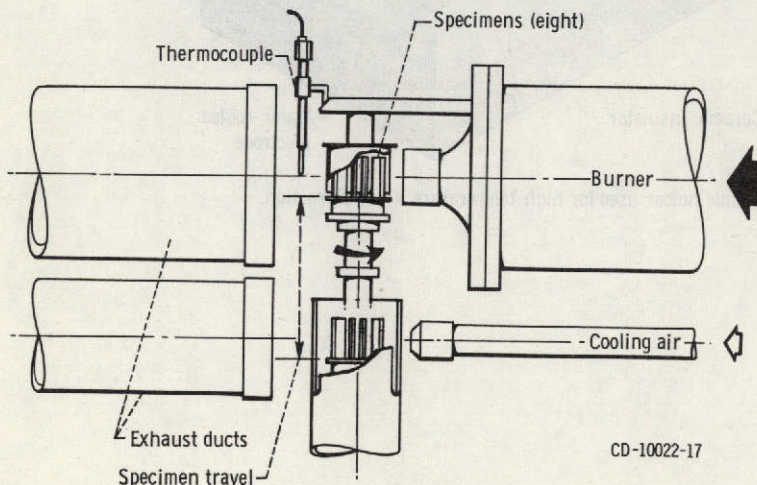
Figure 4. - Sample holder used for high-temperature X-ray diffraction.





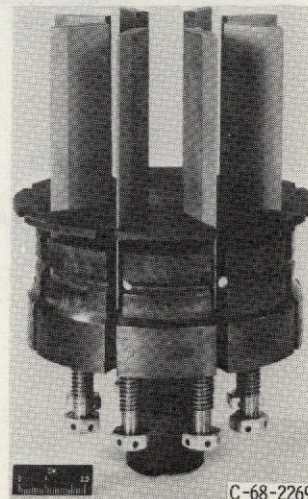
C-68-2003

(a) Overall view.



CD-10022-17

(b) Schematic diagram.



C-68-2269

(c) Specimen holder assembly.

Figure 5. - High-gas-velocity oxidation apparatus.

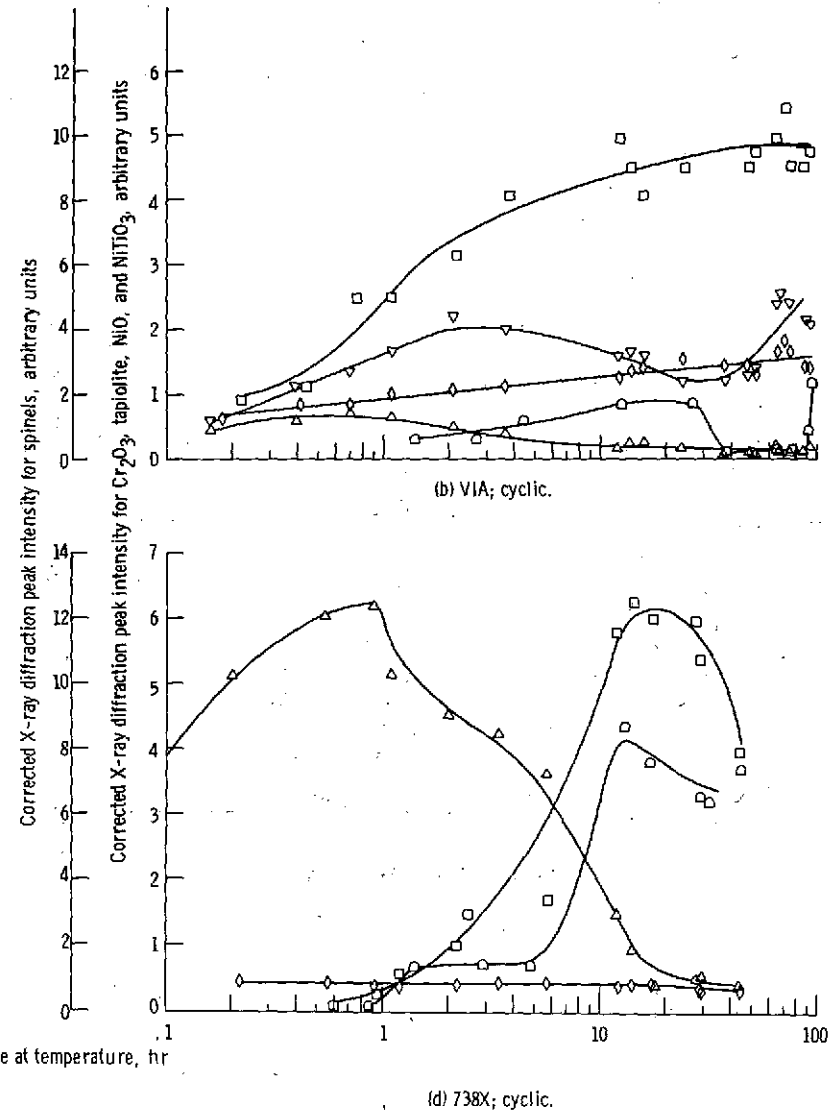
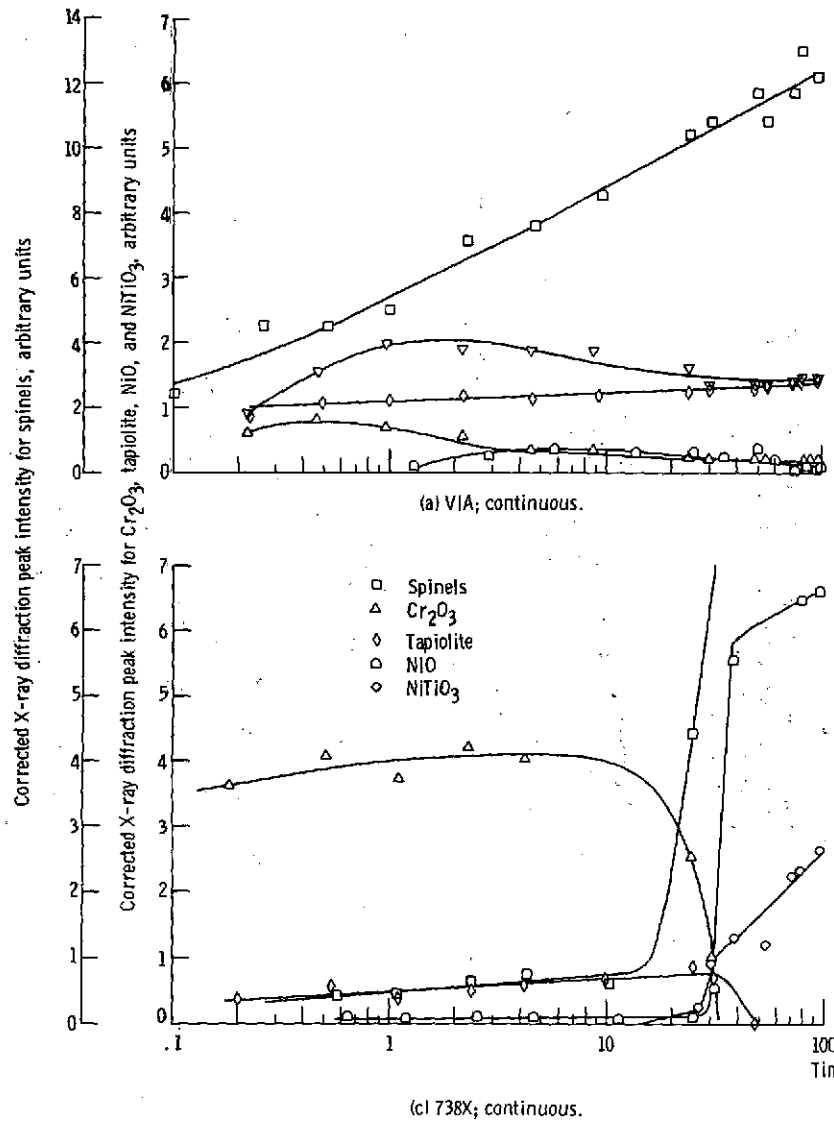


Figure 6. - Effect of continuous and cyclic oxidation at 1100°C on oxides formed on VIA and 738X. Convection flow only (from ref. 5).

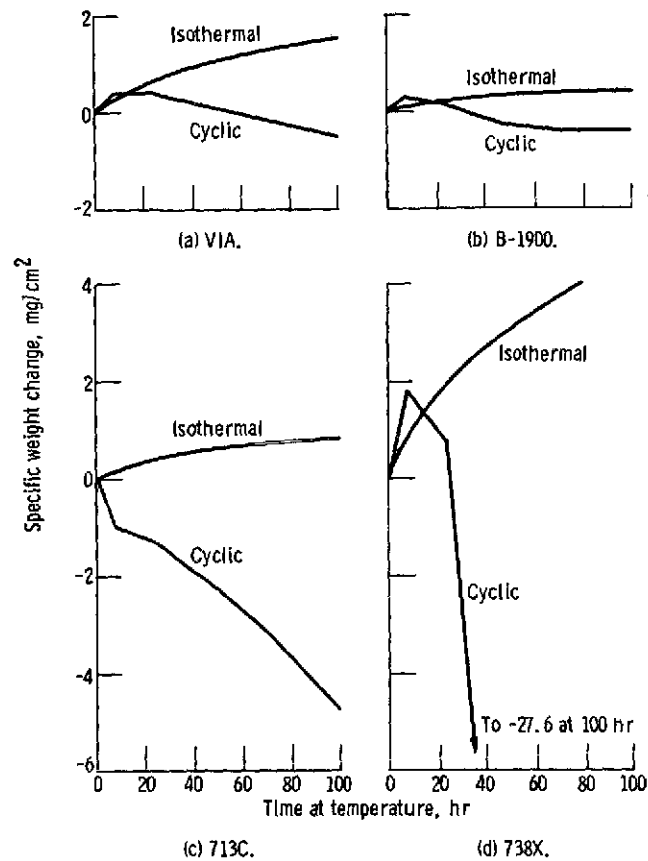


Figure 7. - Static-air cyclic and isothermal oxidation at 1100° C. Each cycle consisted of 1 hour at temperature and 40 minutes of cooling; isothermal values at temperature, cyclic values after cooling.

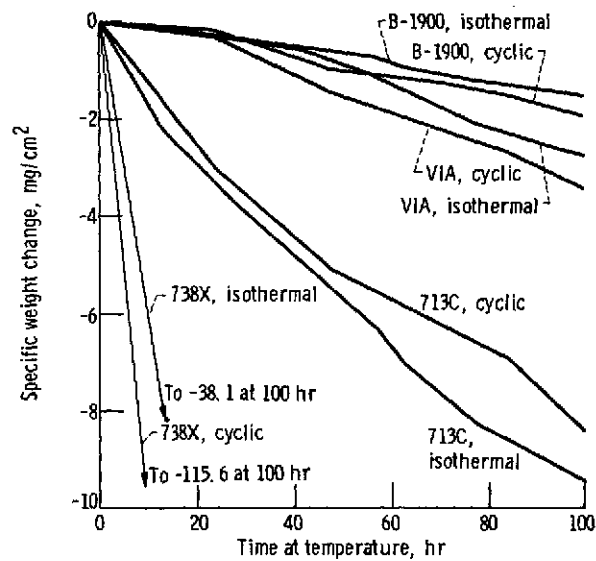


Figure 8. - High-velocity oxidation of VIA, B-1900, 713C, and 738X at 1100° C. Cyclic and isothermal; cycles were 1 hour at temperature and 40 minutes of cooling.



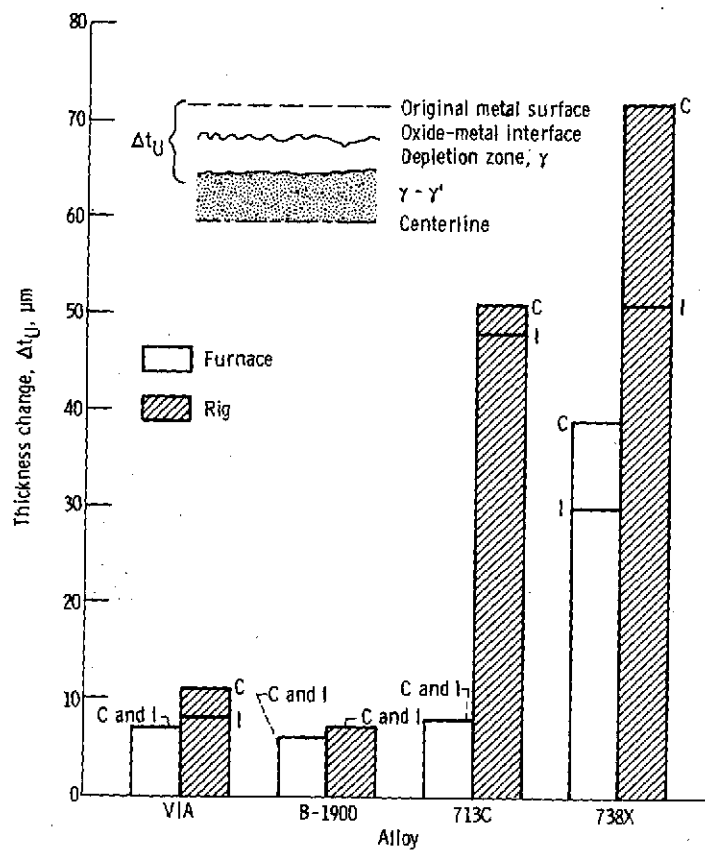


Figure 9. - Cyclic and isothermal oxidation of four superalloys after 100 hours at 1000° C as determined from affected metal. Isothermal, I; cyclic, C.

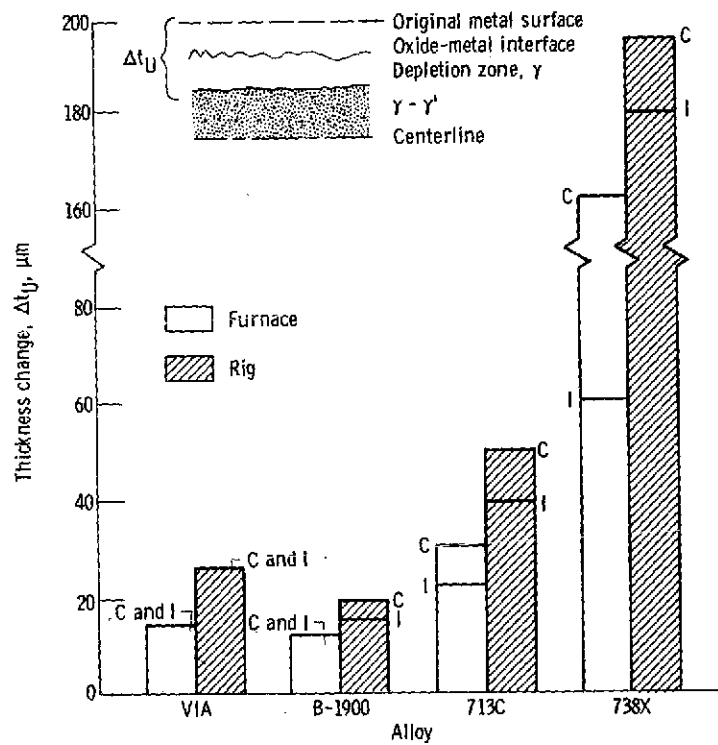
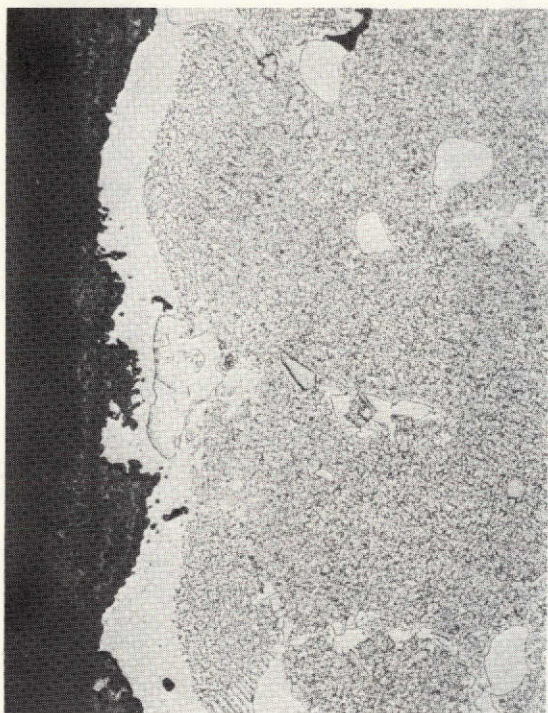
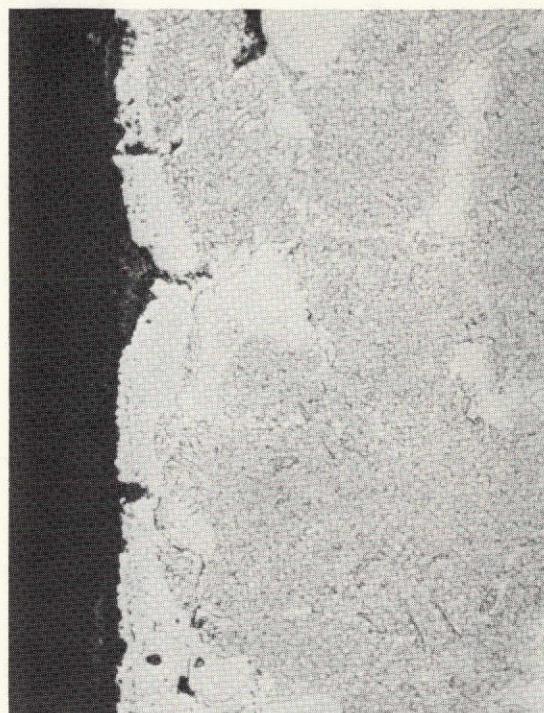


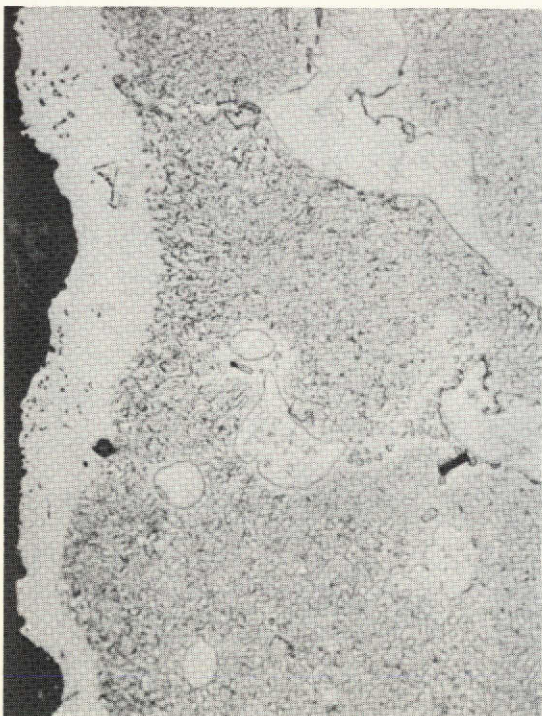
Figure 10. - Cyclic and isothermal oxidation of four superalloys after 100 hours at 1100°C as determined from affected metal. Isothermal, I; cyclic, C.



(a) Isothermal furnace.



(b) Cyclic furnace.



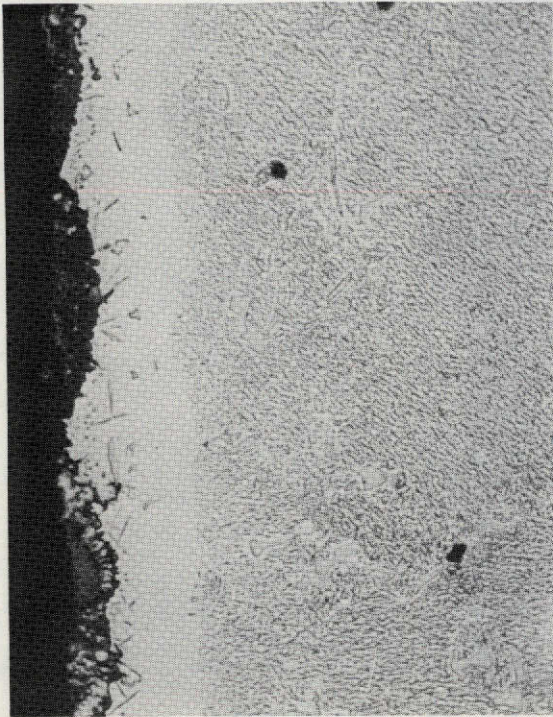
(c) Isothermal burner rig.



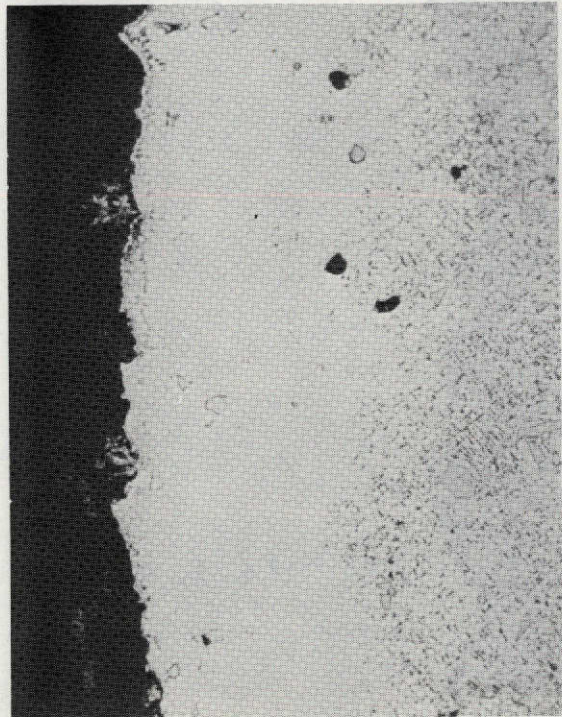
(d) Cyclic burner rig.

Figure 11. - Effect of test conditions on microstructure of VIA oxidized for 100 hours at 1100° C. Etched, X250.





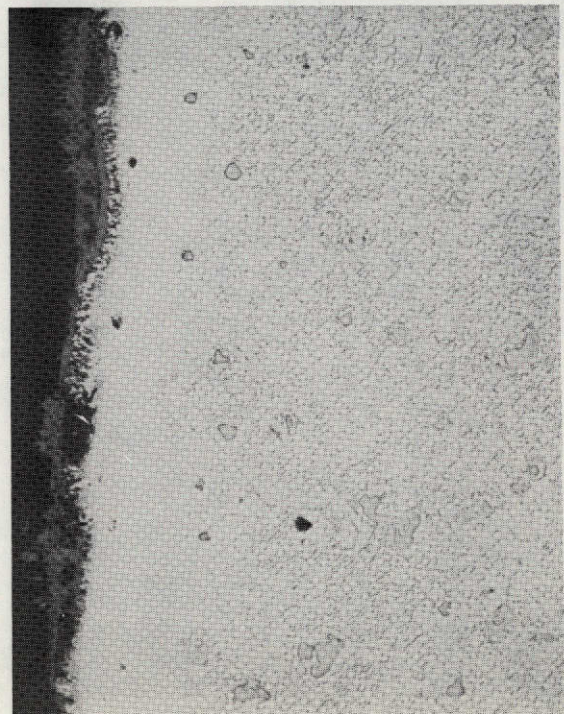
(a) Isothermal furnace.



(b) Cyclic furnace.



(c) Isothermal burner rig.



(d) Cyclic burner rig.

Figure 12. - Effect of test conditions on microstructure of 738X oxidized for 100 hours at 1100° C. Etched. X250.



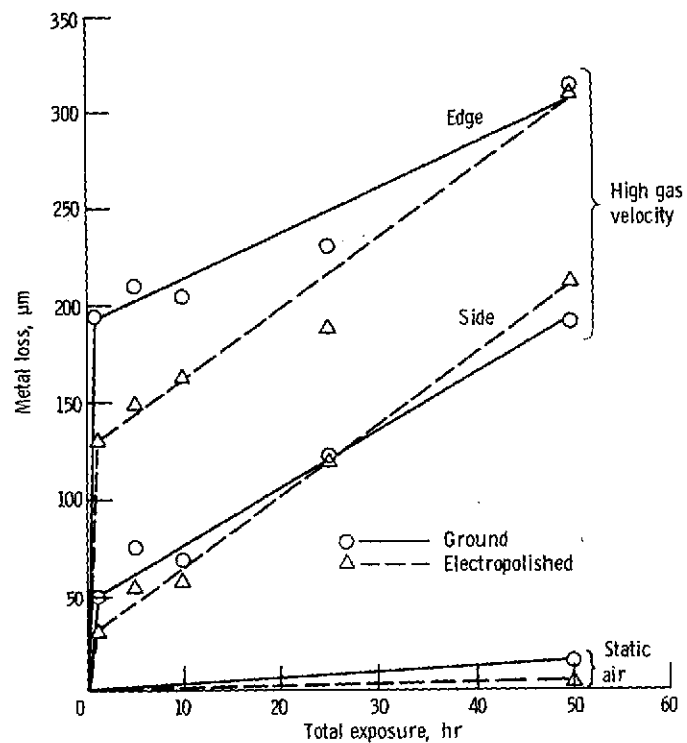


Figure 13. - Comparison of metal loss in ground and electropolished TD NiCr exposed to high-gas-velocity oxidation at 1204° C (2200° F) and static-air oxidation at 1200° C (2192° F).